HHS Public Access

Author manuscript

Genesis. Author manuscript; available in PMC 2017 January 08.

Published in final edited form as:

Genesis. 2016 January ; 54(1): 38–52. doi:10.1002/dvg.22911.

Generation of an estrogen receptor beta-iCre knock-in mouse

Joseph A Cacioppo[1], **Yongbum Koo**[1,2], **Po-Ching Patrick Lin**[1], **Sarah A Osmulski**[1], **Chunjoo D Ko**[1], and **CheMyong Ko**[1,*]

[1]Comparative Biosciences, College of Veterinary Medicine, University of Illinois, Urbana-Champaign, IL 61802, USA

[2]School of Biological Sciences, Inje University, Gimhae, South Korea

Abstract

A novel knock-in mouse that expresses codon-improved Cre recombinase (iCre) under regulation of the estrogen receptor beta (*Esr2*) promoter was developed for conditional deletion of genes and for the spatial and/or temporal localization of *Esr2* expression. ESR2 is one of two classical nuclear estrogen receptors and displays a spatio-temporal expression pattern and functions that are different from the other estrogen receptor, ESR1. A cassette was constructed that contained iCre, a polyadenylation sequence, and a neomycin selection marker. This construct was used to insert iCre in front of the endogenous start codon of the *Esr2* gene of a C57BL/6J embryonic stem cell line via homologous recombination. Resulting Esr2-iCre mice were bred with ROSA26-lacZ and Ai9-RFP reporter mice to visualize cells of functional iCre expression. Strong expression was observed in the ovary, the pituitary, the interstitium of the testes, the head and tail but not body of the epididymis, skeletal muscle, the coagulation gland (anterior prostate), the lung, and the preputial gland. Additional diffuse or patchy expression was observed in the cerebrum, the hypothalamus, the heart, the adrenal gland, the colon, the bladder, and the pads of the paws. Overall, Esr2-iCre mice will serve as a novel line for conditionally ablating genes in *Esr2*-expressing tissues, identifying novel *Esr2*-expressing cells, and differentiating the functions of ESR2 and ESR1.

Keywords

Estrogen receptor beta; Esr2-iCre; Cre recombinase; Knock-in; Granulosa cells

Introduction

Estrogens, and 17β-estradiol (E2) in particular, are a group of important steroid hormones in the human body with a plethora of functions in nearly all organs. Estrogens act primarily through their two cognate receptors, estrogen receptors alpha and beta. Estrogen receptor beta (ESR2, also ER[b], ERbeta, Estrb, ERβ) is a classic nuclear receptor (Tremblay *et al.*,

*Corresponding author: CheMyong Ko, Ph.D., Department of Comparative Biosciences, College of Veterinary Medicine, University of Illinois at Urbana-Champaign, 3806 VMBSB, MC-002, 2001 South Lincoln Avenue, Urbana, IL 61802, USA, 217-333-9362 (office), 217-244-1652 (fax), jayko@illinois.edu.

Disclosure: The authors have nothing to disclose.

1997) with widespread expression throughout the body. The mRNA for *Esr2* has been found at high levels in the ovary, prostate, and hypothalamus with expression also seen in the testis, uterus, bladder, and lung (Karolczak and Beyer, 1998; Kuiper *et al.*, 1997; Kuiper and Gustafsson, 1997). ESR2 also plays a prominent role in many cancers, including the breast, bladder, and ovary (Drummond and Fuller, 2012; Yu *et al.*, 2011). Additionally, ESR2 has been found to play a critical role specifically within the granulosa cells of the ovary for successful ovulation (Dupont *et al.*, 2000). Mice that lack ESR2 give birth to fewer and smaller litters (Krege *et al.*, 1998) that are the result of aberrant expression of over 300 genes in the granulosa cells (Binder *et al.*, 2013). These mice also develop bladder and prostate hyperplasia in old age, though future work on the exact pathways underlying ESR2-regulated anti-proliferation remains. Current available mouse models to examine ESR2 include one commercially available (Jackson Laboratories, Bar Harbor, ME) global *Esr2* knockout (KO) that was generated by neomycin cassette insertion (Krege *et al.*, 1998) and one mouse line with a floxed 3rd exon of the *Esr2* gene (Binder *et al.*, 2013). However, no models exist for conditional deletion of genes localized to *Esr2*-expressing cells. Therefore, this study aimed to create a novel knock-in mouse that expresses codon-improved Cre recombinase (iCre) under the *Esr2* promotor for conditional gene deletion and localization of global *Esr2* expression. It was hypothesized that this mouse would serve as a novel tool for gene ablation specifically within the granulosa cells of the ovary, and that it would be an alternative to previous granulosa cell-specific Cre lines (Bertolin *et al.*, 2014; Fan *et al.*, 2008). This mouse would be particularly useful for cell lineage-tracing experiments as iCre would permanently ablate floxed genes in *Esr2*-expressing cells, allowing for permanent removal of genes from the time of *Esr2* expression onward. Such ablation would begin at the earliest time of endogenous *Esr2* expression and persist for the duration of Esr2 expression, in contrast to an inducible-Cre mouse line that would offer experimental control of Cre induction and subsequent gene ablation. In order to visualize localization of *Esr2* expression, Esr2-iCre mice were crossed with two lines of reporter mice: ROSA26-lacZ (Soriano, 1999) and Ai9-RFP mice (Madisen *et al.*, 2010). This novel animal model will be an important and useful new tool for the study of ESR2 itself and the genes that are active in the ESR2-expressing cells.

METHODS

Ethics Statement

This study was carried out in tight accordance with the recommendations in the Guide for the Care and Use of Laboratory Animals of the National Institutes of Health. Animal protocols were approved by the University of Illinois Animal Care and Use Committee (Protocols: 11205 and 14222), and all efforts were made to minimize animal suffering. Animal models generated in this study will be made readily available to the research community.

Targeting Vector Construction

An iCre-polyA-FRT-neo-FRT cassette (3266 bp) was generated from a pBluescript KS(+)-iCre plasmid, similar to a previous transgenic study (Cacioppo *et al.*, 2015) and was modified for insertion into the mouse *Esr2* gene. The cassette was inserted before the

translational initiation codon of the *Esr2* gene of a BAC clone (ID RP23-342B14) that was purchased from Invitrogen (Carlsbad, CA) by recombineering according to protocols provided by Frederick National Laboratory for Cancer Research (Jahrling *et al.*, 2014; Parkitna *et al.*, 2009; Thomason *et al.*, 2014). Briefly, a homology arm (upstream from ATG at exon 2) was amplified using primer pairs (5'-CGTCGACAAGGCCTCTCGAGCCTC-3', 5'-CGAATTCGAATTAAAAAACCTCCCACACCTC-3') and cloned between the *Eco*R1 site and the *Sal*1 site upstream of the cassette. Another homology arm downstream from ATG was amplified using primer pairs (5'-AGGATCCGGAATAGTAACTTCTCCATGGTAG-3', 5'-CGCGGCCGCGATGTGCTGCAAGGCGATTAAG-3') and cloned the between *Bam*H1 site and the *Not*1 site after the cassette. The cassette with the two homologies was cut with *Eco*R1 and *Not*1, gel purified, introduced into *E. coli* SW106 (heat-induced) carrying the BAC for insertion. Engineered BAC clones were selected on LB plate supplemented with kanamycin (25 mg/liter). The engineered *Esr2* gene was retrieved in a pL253 targeting vector. Briefly, an upstream homology arm (*Not*1/*Hin*dIII fragment) which was amplified with primer pairs (5'-GACGCGTAGACTGCATCTCTGTAGTCCAA-3' and 5'-GAAGCTTGATGCTCTCAGAGACTCACG-3') and a downstream homology arm (*Hin*dIII/*Spe*1 fragment) which was amplified with the primer pairs (5'-AGGCCGAGGCGGCCATGTCCATCTGTGCCTCCTCT-3' and 5'-AGACGTCAACACTGTAGTTCATCACAGCAG-3') were cloned between *Not*1 site and *Spe*1 site of pL253. The resulting plasmid was linearized by *Hin* dIII digestion and introduced into *E. coli* SW106 (heat-induced) carrying the engineered BAC. Retrieved clones were selected on LB medium supplemented with ampicillin (50 mg/liter). The targeting vector was linearized by *Cla* 1 digestion and used for embryonic stem (ES) cell targeting.

Gene Targeting

The cassette was then inserted into the genome of embryonic stem (ES) cells at the University of Illinois at Urbana-Champaign Biotechnology Center. C57BL/6N-PRX-B6N #1 mouse black ES cells were purchased from Jackson Laboratory (Bar Harbor, Maine) and maintained in media according to the supplier's instructions. ES cells received cassette DNA through electroporation and homologous recombination at 75% confluence, and were then grown in selection media with G418 (200μg/ml). ES cell DNA was extracted and sent to the Murine Genetic Analysis Laboratory at the University of California Davis. Quantitative PCR, long range PCR, karyotyping, and viral screening were performed on 288 ES cell clones to ensure insertion of a single copy in the correct orientation without defect. Long range PCR was performed on the 5' end with primers LR-F1 and LR-vR (5'-TGAGATCTAGGTTCAGAAGGAGAAGG-3' and 5'-GGTGCACAGTCAGCAGGTTGGAG-3') to produce 3,352bp DNA fragments, and on the 3' end with primers LR-vF and LR-R1 (5'-CTGTCCTTGATCCCTTCTCTGTGC-3' and 5'-CGCATCGCCTTCTATCGCCTTC-3') to produce 3,506 bp DNA fragments. Six ES cell clones were identified as correctly targeted. Selection copy number analysis was performed based on the neomycin insertion sequence to ensure no additional cassette copies were present. Cells of one of these lines (#030) were expanded and used to generate black and

white chimeric mice by injecting them into blastocysts that were retrieved from C57BL/6J albino mice at the University of Illinois Biotechnology Center.

Animals Used

Eight chimeric male mice containing the Esr2-iCre construct that were at least 50% black in color were produced from surrogate mothers. Five chimeras were bred with albino WT C57B/6J female mice. The genotype of their offspring was determined by PCR of ear tissue using primers iCre-F (5′-TCTGATGAAGTCAGGAAGAACC-3′) and iCre-R (5′-GAGATGTCCTTCACTCTGAATC-3′) (Bridges *et al.*, 2008) to detect iCre presence. The three-primer set 5'-CAGGTGCTGTTGGATGGTCTTC-3', 5'-CTTAGTTACTCCGGCAGCTTGAAC-3', and 5'AGGGGAAGTAAGGCTTGATGGTGA-3' was later used to determine if mice were hetero- or homozygous for Esr2-iCre. The 3rd female chimera gave birth to a litter of normal size with eight pups, of which four pups were black in color and all four were globally positive for the iCre gene. Given its normal fecundity and successful gene transmission, this mouse line was chosen for removal of the neomycin targeting cassette and subsequent breeding with reporter lines. These mice were first bred with B6N.Cg-Tg(ACTFLPe)9205Dym/CjDswJ (FLP) mice (Jackson Laboratory) to remove neomycin, and then backcrossed with wild type (WT) mice to remove the FLP gene (Rodriguez *et al.*, 2000). FLP presence was determined with the primers 5'-AACGGAACAGCAATCAAGAGAGCC-3' and 5'-TGCTTCTTCCGATGATTCGAACTG-3'. For characterization of expression, Esr2-iCre mice were bred with two reporter lines: B6;129S4-*Gt26Sor*^{tm1Sor}/J (ROSA26) reporter mice to visualize expression by X-gal staining (Soriano, 1999), and B6;129S6-*Gt26Sor*$^{tm9(CAG\text{-}tdTomato)Hze}$/J (Ai9) reporter mice (Madisen *et al.*, 2010) to visualize expression by presence of red fluorescent protein (RFP). Of note, cells that are positive by X-gal staining or RFP presence may be either cells that positively express iCre or cells that are progeny of those that have previously expressed iCre. Lastly, expression of *Esr2* and *iCre* were compared between WT, heterozygous, and homozygous Esr2-iCre mice.

Characterizing Esr2-iCre Expression

Tissues were collected and washed two times in cold phosphate buffered saline (PBS). For X-gal staining, tissues were incubated in 4% paraformaldehyde (PFA) on ice for one hour. After again washing twice with PBS, the tissues were placed in individual vials of X-gal (5-bromo-4-chloro-3-indolyl-β-D-galactopyranoside) or Red-gal (6-chloro-3-indolyl-beta-D-galactopyranoside, also known as Salmon-gal or Magenta-gal) staining solution (Millipore Specialty Solutions, Billerica, MA). Tissues were then placed on a shaker and incubated for 24-48 hours in the dark at 4°C. Following incubation, tissues were washed three times with PBS, and then incubated in the dark for one hour at room temperature in X-gal holding solution (Millipore) before being re-fixed overnight in 4% PFA at 4°C. After fixation, gross images were taken of the tissues before tissues were dehydrated and embedded in paraffin blocks. Blocks were sectioned at 5μm thickness using the microtome. Slides were then counter-stained with nuclear fast red (Fisher Scientific, Pittsburg, PA) and imaged with an Olympus BX51 microscope. For RFP signal visualization, gross images were taken using a Zeiss SV11 fluorescent microscope immediately after euthanasia. Tissues were then fixed

overnight in 4% PFA, embedded in paraffin, and serially sectioned at 5μm, or were frozen immediately after collection in ethanol and dry ice and were then sectioned at 7μm. Using an Olympus BX51 microscope, raw sections were used for fluorescence visualization; adjacent slides were stained with hematoxylin and eosin (Thermo Scientific, Kalamazoo, MI) to histologically confirm structures.

Comparing Esr2 and iCre Expression in Heterozygous and Homozygous Esr2-iCre Mice

Semi-quantitative RT-PCR was performed to determine if *Esr2* expression was globally removed from homozygous mice, and if there was a difference in *Esr2* or *iCre* expression in heterozygotes. RT-PCR was performed on tissues from homozygous Esr2-iCre mice, heterozygous Esr2-iCre mice, and wild type mice using 5'-GAC GAA GAG TGC TGT CCC AA-3' and 5'-TCA GCT TCC GGC TAC TCT CT-3' for *Esr2* (209bp), the above primers for iCre (500bp), and 5′-CCTGAAGGTCAAAGGGAATGTG-3′ with 5′-GTCTGCCTTCAGCTTGTGGAT-3′ to produce a 79 basepair for *Rpl19* as a housekeeping gene. RNA was extracted using Trizol® solution (Ambion, Carlsbad, CA), and then purified with a Qiagen RNEasy Kit (Valencia, CA). RNA was analyzed by a Nanodrop machine for quantity and purity. Complementary DNA was then generated by M-MLV Reverse Transcriptase using random primers. Template RNA quantities were normalized prior to reverse transcription. Amplified DNA (4.0 μL) was visualized on a 2.0% agarose gel and was quantified using ImageJ freeware (NIH, Bethesda, MD) to measure peak pixel grayscale levels within the defined areas of the bands.

Statistical Analysis

Data analyses were performed using statistical software (SPSS, Inc., released 2013, PASW Statistics for Windows, Version 22.0, Chicago, IL). Continuous data were tested for normal distribution by a Shapiro-Wilk test. All normally distributed continuous data were analyzed with parametric tests (ANOVA) and a Bonferroni *post hoc* test. All non-normally distributed continuous data were analyzed by non-parametric tests (Kruskal Wallis ANOVA). Data are graphically presented as the mean and standard error of the mean. For all analyses the alpha value was set to 0.05.

RESULTS AND DISCUSSION

The goal of this study was to generate a novel mouse line that faithfully expresses codon-improved Cre recombinase in the same cells as endogenous estrogen receptor beta (*Esr2*) expression. Generation of a knock-in mouse was chosen to ensure that there was little disruption of the *Esr2* promoter. Additionally, while heterozygous mice have a normal phenotype and retain one functional *Esr2* allele, homozygous knock-in mice are global knockouts for the modified *Esr2* gene while retaining the ability to remove floxed genes in *Esr2*-expressing cells. Expression of iCre in place of *Esr2* is useful for both removing genes in *Esr2*-expressing cells as well as visually characterizing areas of *Esr2* expression.

To generate this mouse model, a bacterial artificial chromosome containing a portion of the *Esr2* gene sequence was purchased as a vector for genetic modification. A cassette containing iCre, a polyadenylation sequence, and an FRT-neomycin-FRT selection marker

was generated using PCR to introduce digestion sites with ensuing endonuclease digestion and end joining. The cassette was then inserted into exon 2 of the *Esr2* gene (Figure 1A). The second exon encodes the central C domain of estrogen receptor beta, the DNA binding domain, which is involved in both binding DNA and receptor dimerization and is highly conserved between estrogen receptors alpha and beta (Zhao *et al.*, 2008). To insert the iCre cassette into exon 2 of the *Esr2* gene within the BAC clone, two homology arms were amplified from the endogenous *Esr2* gene by PCR and joined on either side of the cassette after restriction enzyme digestion, resulting in a total length of 10,853 base pairs. The pL253 plasmid was used for ampicillin-dependent retrieval after homology arm insertion (Figure 1B). The plasmid was linearized by *Cla1* digestion and the cassette was inserted into C57BL/6J black embryonic stem cells by homologous recombination. The ES cell clones that possessed the targeting construct insertion were sent to the Murine Genetic Analysis Laboratory at the University of California Davis to identify correctly targeted clones (Figure 1C). Six ES cell clones were found to have a correctly inserted targeting sequence. Among them, one ES cell colony (#30) was selected for blastocyst injection and chimera generation. One chimera gave birth to a normal number of black pups that were positive for the iCre gene. These offspring were then bred with a FLP mouse to remove the neomycin targeting vector; their pups were crossed with WT C57Bl/6 mice to generate the final knock-in Esr2-iCre mouse line that lacks the neomycin portion of the cassette (Figure 1A, bottom).

Mouse breeding was performed using one mouse heterozygous for Esr2-iCre to avoid homozygote Esr2-knockout mouse generation. Mice that are heterozygous for Esr2-iCre have lost one functional *Esr2* allele; however, this is expected to have little or no impact on reproductive parameters as global Esr2-KO mice are fertile (Drummond and Fuller, 2010). The Esr2-iCre mice were crossed with homozygous ROSA26 and Ai9 reporter mice, which produce beta-galactosidase and red fluorescent protein (RFP), respectively, in cells or cell lineages of iCre expression. Esr2-iCre ROSA26 mice and Esr2-iCre Ai9 showed identical reporter expression in tissues examined and otherwise maintained normal phenotypes and fertility.

To characterize expression, adult mice were collected at 2-4 months of age and examined for X-gal staining or RFP expression. Mice were first examined as a whole during dissection, then on the individual organ level, and lastly histologically. Wild-type (WT) mice were sacrificed and imaged as negative controls: no fluorescence was observed grossly in WT mice and only faint background was observed histologically in unstained sections. However, it was observed that WT tissues that were fixed for more than 24 hours in paraformaldehyde (PFA) were subject to increased auto-fluorescence grossly and histologically. Similar increased auto-fluorescence was observed in tissues that were in 70% ethanol for extended periods of time (>2 months). Histological auto-fluorescence could be quenched by quickly staining with Sudan Black B solution (CAS 4197-25-5, Santa Cruz; data not shown), though this also diminishes any normal RFP signal. X-gal staining produced significant background when tissues were stained above room temperature or for longer than 48 hours.

The primary interest in generating Esr2-iCre mice was as a tool for the ablation of ovarian genes, specifically within the granulosa cells. Expression of *Esr2* has been well characterized in granulosa cells of growing follicles beginning in the primary follicle stage

(Byers *et al.*, 1997; Jakimiuk *et al.*, 2002; Sar and Welsch, 1999; Shughrue *et al.*, 1998). Expression of *Esr2* has been controversial in the oviduct, with rodent and sheep models reporting little to no expression in the adult female reproductive tract outside of the oviduct (Cardenas and Pope, 2012; Sar and Welsch, 1999), while hormone-dependent expression has been reported in the bovine oviduct (Ulbrich *et al.*, 2003). In the immature uterus, expression of *Esr2* has been reported in both the epithelium and the stroma of the mouse (Weihua *et al.*, 2000), while in adults, expression is localized in the glandular epithelial cells (Hiroi *et al.*, 1999) where it is believed to play a role in modulation of ESR1 activity (Weihua *et al.*, 2000) and also likely to the stroma during days 7-15 of pregnancy (Minorics *et al.*, 2004).

In Esr2-iCre Ai9 mice, RFP was noted grossly in the ovary, oviduct, and uterus (Figure 2). A similar pattern was seen in Esr2-iCre ROSA26 mice (Supplemental Figure 1). Fluorescence/staining was most notable from the ovary, where it was present throughout the granulosa cells as well as the theca cells and stroma cells. The oviduct demonstrated punctate expression in some of the epithelial cells, particularly concentrated towards the ampulla and away from the isthmus. Spotted expression was also observed in a few cells of the muscularis layer about the oviduct. In the uterus, cells demonstrating RFP expression were present throughout the epithelium, and also in a few stroma cells of the endometrium and myofibrils of the myometrium (Figure 2). The presence of fluorescence and staining within the theca and stroma cells suggests that ovarian *Esr2* expression may be active in these areas during development in ovarian precursor cells, or at low levels in the adult ovary. Evidence of this is shown by differences in staining between PND21 and PND66 Esr2-iCre ROSA26 female mice (Supplemental Figure 1). Post-natal day 21 staining showed distinct staining surrounding the follicle with no visible staining in the oviduct or uterus. Meanwhile, day 66 mice showed darkened staining throughout the entire ovary as well as punctate staining in the oviduct and uterus. This difference indicates that *Esr2* is expressed at varying time points during development and explains why fluorescence and staining were visible in the theca and stroma of the ovary in mice 2-4 months of age or older. It is possible that *Esr2* expression in the oviduct is under hormonal regulation, as seen in the cow where expression peaks during the luteal phase (Ulbrich *et al.*, 2003) and originally hypothesized by Mowa and Iwanaga (Mowa and Iwanaga, 2000). Future ovariectomy experiments utilizing Cyp19-knockout mice may determine if changes in expression during aging are the result of estrogenic changes, which is likely, or instead arise from another stimulus during the aging process such as a non-ovarian hormone.

Unexpectedly, we found that three of 21 pups born to Esr2-iCre ROSA26 female mice were globally positive to X-gal staining or RFP, indicating a global expression of iCre (Supplemental Figure 2). Interestingly, Esr2-iCre ROSA26 mice that displayed such global expression were all born to mothers that carried the Esr2-iCre allele. When the Esr2-iCre allele was inherited from the paternal line, no Esr2-iCre ROSA26 mouse had global reporter expression. Therefore, the global expression was most likely due to a functional iCre expression in the oocytes. This correlates well to the 5% of oocytes that demonstrate positive reporter expression in adult female ovaries (Figure 2). In support of this reasoning, presence of *Esr2* transcript has been reported in the oocytes of several mammalian species

(Bocca *et al.*, 2008; Hulas-Stasiak and Gawron, 2007; Juengel *et al.*, 2006). The origin of the *Esr2* transcript in the oocyte is currently unknown; it may be expressed by the oocyte itself or cumulus granulosa cells and then transported to the oocyte. It is well established that cumulus granulosa cells of the ovary pass maternal mRNA to the oocyte (Macaulay *et al.*, 2014; Wigglesworth *et al.*, 2013). In support, *Esr2* is highly expressed in the granulosa cells (Byers *et al.*, 1997; Jakimiuk *et al.*, 2002; Sar and Welsch, 1999; Shughrue *et al.*, 1998). Therefore, it is possible that iCre expression and ROSA26 activation occurs in some but not all oocytes due to exchange of maternal Esr2 mRNA between the granulosa cells and the oocyte. Future users of this mouse line are advised to use Esr2-iCre-carrying males and wild-type females as breeders.

In the adult male reproductive tract, multiple tissues demonstrated red fluorescence/staining, including the testes, epididymis, ductus deferens, coagulation gland (anterior prostate), and prepucial glands (Figure 3, Supplemental Figure 3). In the testes, RFP was present in the interstitium between the seminiferous tubules. This pattern has been previously reported (van Pelt *et al.*, 1999), though expression has also been reported in the Sertoli cells and germ cells. However, Sertoli expression was not observed. Further, germ cell expression was not observed, either in the spermatogonia or spermatids of the testes, or in the sperm themselves visible throughout the epididymis; no pups were born with global RFP expression to Esr2-iCre males. This is partially similar to more recent reports of human *Esr2* expression where it was observed in Leydig cells and peritubular myoid cells, though also in germ cells (Shapiro *et al.*, 2005). Punctate staining was present throughout the epithelium of the rete testes, the head of the epididymis, and the tail of the epididymis, but not the body of the epididymis (Figure 3). Similarly, expression was seen in the epithelium of the vas deferens as well. These data are similar to previous reports using immunohistochemical localization (Choi *et al.*, 2001; Hess *et al.*, 1997; Shapiro *et al.*, 2005). Overall, differences in male gonadal expression of *Esr2* between Esr2-iCre mice and previous reports may be the result of species differences between human and mouse, between mouse strains, or as a consequence of construct insertion. The Esr2-iCre mouse line should be utilized with confirmatory protein-detection in WT mice if used in the future for examination of male gonadal tissue, gamete development, and gamete storage or maturation.

In addition to a superfluity of other functions, the pituitary and brain (specifically the hypothalamus) are important in reproductive regulation and hormonal feedback loops in both genders. Not surprisingly, both organs had presence of red fluorescence or staining in each gender (Figure 4, Supplemental Figure 4). Expression in the brain and pituitary was similar between genders in adult mice. In the brain, diffuse fluorescence was grossly present throughout the cerebrum, though it was absent in the hindbrain, the cerebellum, and the optical tracts. More marked fluorescence was grossly visible in the hypothalamus. Points of increased fluorescence were also present on the ventral cerebrum, which may represent the Islands of Calleja, a portion of the limbic system (Adjei *et al.*, 2013). Previous reports on *Esr2* expression in the brain have demonstrated expression in the olfactory bulb, the amygdaloid nucleus, the medial geniculate nucleus, the posterior hypothalamic nucleus, and the suprachiasmatic nucleus, which are estrogen-dependent (Yamaguchi and Yuri, 2014).

The data presented confirm previous findings, and also implicate additional *Esr2* expression throughout neurons of the cerebrum.

Previous studies have also reported pituitary expression of *Esr2*. In fetal rats, ESR2 is present within the developing pituitary from post-natal day 12 (PND12) onward, though expression decreases in the adult and is then limited to the periphery and area adjacent to the intermediary lobe, with no differences between genders (Nishihara *et al.*, 2000). The data confirm previous findings regarding limited expression in the anterior pituitary near the intermediary lobe (Supplemental Figure 4). However, strong fluorescence within the posterior pituitary was also observed in contrast to previous reports of ESR2 protein expression (Nishihara *et al.*, 2000). This may be reflective of developmental expression in the posterior pituitary, especially as these cells are descended from the developing hypothalamus where *Esr2* expression has been previously observed.

Beyond the reproductive organs, *Esr2* has a widespread distribution throughout the body and has also been implicated in multiple types of cancer as well (Castiglione *et al.*, 2008; Elicevik *et al.*, 2006; Kalbe *et al.*, 2007; Lamote *et al.*, 2007; Pelzer *et al.*, 2005; Valimaa *et al.*, 2004; Vanderhorst *et al.*, 2005; Wu *et al.*, 2005). Global survey of Esr2-iCre mice identified RFP in multiple organs (Figure 4). In particular, RFP was diffusely present in the detrusor muscle of the bladder, in several cells in a spotted pattern in the mucosa of the colon (but very limited in the gut-associated lymphatic tissues therein), in the most interior layer of the central cornea of the eye, in the epicardium and atrial myocardium, throughout the entirety of the lung, in some acini of the pancreas, in the some serous cells of the acini of the salivary glands, and throughout the skeletal muscle fibers (Figure 4). A detailed list of all organs examined, as well as previous related literature, is presented in Table 1. Future characterization may specifically identify the cell types or timing of expression within these non-reproductive tissues.

Lastly, global loss of *Esr2* expression was confirmed in Esr2-iCre/iCre mice. These animals were generated by crossing Esr2-iCre male and female mice. Previous studies indicate that loss of both *Esr2* alleles results in fewer litters and fewer pups per litter, with fewer antral follicles and fewer corpora lutea in the ovaries (Drummond and Fuller, 2010), but possessing a single functional allele is expected to be sufficient to restore function. RT-PCR for *Esr2*, *iCre*, and *Rpl19* expression revealed that Esr2-iCre homozygous mice have lost all *Esr2* expression in the ovary (Figure 5B,C). However, heterozygote mice had no difference in expression from WT mice. Homozygous Esr2-iCre mice were phenotypically similar to reports of global Esr2-KO mice. These animals had no significant difference in body weight from WT mice and were fertile. However, cyclicity was more irregular than in WT mice, with longer periods of estrus or diestrus in some individuals similar to previous observations (data not shown).

In conclusion, novel knock-in Esr2-iCre mice express Cre recombinase in cells and cell lineages that mimic endogenous *Esr2* expression. Cre activity, examined both by β-galactosidase staining and RFP expression through reporter line crossing, is present throughout the ovary, lungs, and skeletal muscle, and is useful for removing genes early in development. Additional high activity is observed throughout the testicular interstitium, the

head and tail of the epididymis, in the hypothalamus and generally throughout the cerebrum, in the pituitary, and in the coagulation gland. Homozygous Esr2-iCre mice are also useful as global *Esr2* knockout models that retain Cre activity. This new animal model will be useful across multiple fields for better understanding the tissue locations and the specific pathways utilized by estrogen receptor beta signaling or by other genes within *Esr2*-expressing cells.

Supplementary Material

Refer to Web version on PubMed Central for supplementary material.

ACKNOWLEDGEMENTS

The authors thank Dr. Lori Raetzman for ROSA26 reporter mice, Dr. Jing Yang for FLP mice, Red Gal reagent, and support in cassette generation, Dr. Fuming Pan for embryonic stem cell DNA insertion and generation of chimeric mice, Stephanie Martynenko for tissue collection, and Karen Doty for histological assistance.

This work was supported by NIH (HD071875 to CK).

REFERENCES

Adjei S, Houck AL, Ma K, Wesson DW. Age-dependent alterations in the number, volume, and localization of islands of Calleja within the olfactory tubercle. Neurobiol Aging. 2013; 34:2676–2682. [PubMed: 23796661]

Bertolin K, Gossen J, Schoonjans K, Murphy BD. The orphan nuclear receptor Nr5a2 is essential for luteinization in the female mouse ovary. Endocrinology. 2014; 155:1931–1943. [PubMed: 24552399]

Binder AK, Rodriguez KF, Hamilton KJ, Stockton PS, Reed CE, Korach KS. The absence of ER-beta results in altered gene expression in ovarian granulosa cells isolated from in vivo preovulatory follicles. Endocrinology. 2013; 154:2174–2187. [PubMed: 23580569]

Bocca SM, Billiar RB, Albrecht ED, Pepe GJ. Oocytes of baboon fetal primordial ovarian follicles express estrogen receptor beta mRNA. Endocrine. 2008; 33:254–260. [PubMed: 18484193]

Bridges PJ, Koo Y, Kang DW, Hudgins-Spivey S, Lan ZJ, Xu X, DeMayo F, Cooney A, Ko C. Generation of Cyp17iCre transgenic mice and their application to conditionally delete estrogen receptor alpha (Esr1) from the ovary and testis. Genesis. 2008; 46:499–505. [PubMed: 18781648]

Byers M, Kuiper GG, Gustafsson JA, Park-Sarge OK. Estrogen receptor-beta mRNA expression in rat ovary: down-regulation by gonadotropins. Mol Endocrinol. 1997; 11:172–182. [PubMed: 9013764]

Cacioppo J, Koo Y, Lin PC, Gal A, Ko C. Generation and characterization of an Endothelin-2 iCre mouse. Genesis. 2015

Cardenas H, Pope WF. Amounts of an estrogen receptor beta isoform increased in the theca of preovulatory follicles of sheep. Anim Reprod Sci. 2012; 131:143–152. [PubMed: 22464186]

Castiglione F, Taddei A, Rossi Degl'Innocenti D, Buccoliero AM, Bechi P, Garbini F, Chiara FG, Moncini D, Cavallina G, Marascio L, Freschi G, Gian LT. Expression of estrogen receptor beta in colon cancer progression. Diagn Mol Pathol. 2008; 17:231–236. [PubMed: 19034156]

Choi I, Ko C, Park-Sarge OK, Nie R, Hess RA, Graves C, Katzenellenbogen BS. Human estrogen receptor beta-specific monoclonal antibodies: characterization and use in studies of estrogen receptor beta protein expression in reproductive tissues. Mol Cell Endocrinol. 2001; 181:139–150. [PubMed: 11476948]

Drummond AE, Fuller PJ. The importance of ERbeta signalling in the ovary. J Endocrinol. 2010; 205:15–23. [PubMed: 20019181]

Drummond AE, Fuller PJ. Ovarian actions of estrogen receptor-beta: an update. Semin Reprod Med. 2012; 30:32–38. [PubMed: 22271292]

Dupont S, Krust A, Gansmuller A, Dierich A, Chambon P, Mark M. Effect of single and compound knockouts of estrogen receptors alpha (ERalpha) and beta (ERbeta) on mouse reproductive phenotypes. Development. 2000; 127:4277–4291. [PubMed: 10976058]

Elicevik M, Horasanli S, Okaygun E, Badur S, Celayir S. Estrogen receptor beta type in the rat urinary bladder. Arch Androl. 2006; 52:407–410. [PubMed: 16873143]

Fan HY, Shimada M, Liu Z, Cahill N, Noma N, Wu Y, Gossen J, Richards JS. Selective expression of KrasG12D in granulosa cells of the mouse ovary causes defects in follicle development and ovulation. Development. 2008; 135:2127–2137. [PubMed: 18506027]

Hess RA, Gist DH, Bunick D, Lubahn DB, Farrell A, Bahr J, Cooke PS, Greene GL. Estrogen receptor (alpha and beta) expression in the excurrent ducts of the adult male rat reproductive tract. J Androl. 1997; 18:602–611. [PubMed: 9432133]

Hiroi H, Inoue S, Watanabe T, Goto W, Orimo A, Momoeda M, Tsutsumi O, Taketani Y, Muramatsu M. Differential immunolocalization of estrogen receptor alpha and beta in rat ovary and uterus. J Mol Endocrinol. 1999; 22:37–44. [PubMed: 9924178]

Hulas-Stasiak M, Gawron A. Immunohistochemical localization of estrogen receptors ERalpha and ERbeta in the spiny mouse (Acomys cahirinus) ovary during postnatal development. J Mol Histol. 2007; 38:25–32. [PubMed: 17180742]

Jahrling PB, Keith L, St Claire M, Johnson RF, Bollinger L, Lackemeyer MG, Hensley LE, Kindrachuk J, Kuhn JH. The NIAID Integrated Research Facility at Frederick, Maryland: a unique international resource to facilitate medical countermeasure development for BSL-4 pathogens. Pathogens and Disease. 2014; 71:211–216.

Jakimiuk AJ, Weitsman SR, Yen HW, Bogusiewicz M, Magoffin DA. Estrogen receptor alpha and beta expression in theca and granulosa cells from women with polycystic ovary syndrome. J Clin Endocrinol Metab. 2002; 87:5532–5538. [PubMed: 12466349]

Juengel JL, Heath DA, Quirke LD, McNatty KP. Oestrogen receptor alpha and beta, androgen receptor and progesterone receptor mRNA and protein localisation within the developing ovary and in small growing follicles of sheep. Reproduction. 2006; 131:81–92. [PubMed: 16388012]

Kalbe C, Mau M, Wollenhaupt K, Rehfeldt C. Evidence for estrogen receptor alpha and beta expression in skeletal muscle of pigs. Histochem Cell Biol. 2007; 127:95–107. [PubMed: 16897031]

Karolczak M, Beyer C. Developmental sex differences in estrogen receptor-beta mRNA expression in the mouse hypothalamus/preoptic region. Neuroendocrinology. 1998; 68:229–234. [PubMed: 9772337]

Krege JH, Hodgin JB, Couse JF, Enmark E, Warner M, Mahler JF, Sar M, Korach KS, Gustafsson JA, Smithies O. Generation and reproductive phenotypes of mice lacking estrogen receptor beta. Proc Natl Acad Sci U S A. 1998; 95:15677–15682. [PubMed: 9861029]

Kuiper GG, Carlsson B, Grandien K, Enmark E, Haggblad J, Nilsson S, Gustafsson JA. Comparison of the ligand binding specificity and transcript tissue distribution of estrogen receptors alpha and beta. Endocrinology. 1997; 138:863–870. [PubMed: 9048584]

Kuiper GG, Gustafsson JA. The novel estrogen receptor-beta subtype: potential role in the cell- and promoter-specific actions of estrogens and anti-estrogens. FEBS Lett. 1997; 410:87–90. [PubMed: 9247129]

Lamote I, Demeyere K, Notebaert S, Burvenich C, Meyer E. Flow cytometric assessment of estrogen receptor beta expression in bovine blood neutrophils. J Immunol Methods. 2007; 323:88–92. [PubMed: 17451738]

Macaulay AD, Gilbert I, Caballero J, Barreto R, Fournier E, Tossou P, Sirard MA, Clarke HJ, Khandjian EW, Richard FJ, Hyttel P, Robert C. The gametic synapse: RNA transfer to the bovine oocyte. Biol Reprod. 2014; 91:90. [PubMed: 25143353]

Madisen L, Zwingman TA, Sunkin SM, Oh SW, Zariwala HA, Gu H, Ng LL, Palmiter RD, Hawrylycz MJ, Jones AR, Lein ES, Zeng H. A robust and high-throughput Cre reporting and characterization system for the whole mouse brain. Nat Neurosci. 2010; 13:133–140. [PubMed: 20023653]

Minorics R, Ducza E, Marki A, Paldy E, Falkay G. Investigation of estrogen receptor alpha and beta mRNA expression in the pregnant rat uterus. Mol Reprod Dev. 2004; 68:463–468. [PubMed: 15236331]

Mowa CN, Iwanaga T. Developmental changes of the oestrogen receptor-alpha and -beta mRNAs in the female reproductive organ of the rat--an analysis by in situ hybridization. J Endocrinol. 2000; 167:363–369. [PubMed: 11115763]

Nishihara E, Nagayama Y, Inoue S, Hiroi H, Muramatsu M, Yamashita S, Koji T. Ontogenetic changes in the expression of estrogen receptor alpha and beta in rat pituitary gland detected by immunohistochemistry. Endocrinology. 2000; 141:615–620. [PubMed: 10650942]

Parkitna JR, Engblom D, Schutz G. Generation of Cre recombinase-expressing transgenic mice using bacterial artificial chromosomes. Methods Mol Biol. 2009; 530:325–342. [PubMed: 19266340]

Pelzer T, Loza PA, Hu K, Bayer B, Dienesch C, Calvillo L, Couse JF, Korach KS, Neyses L, Ertl G. Increased mortality and aggravation of heart failure in estrogen receptor-beta knockout mice after myocardial infarction. Circulation. 2005; 111:1492–1498. [PubMed: 15781739]

Rodriguez CI, Buchholz F, Galloway J, Sequerra R, Kasper J, Ayala R, Stewart AF, Dymecki SM. High-efficiency deleter mice show that FLPe is an alternative to Cre-loxP. Nat Genet. 2000; 25:139–140. [PubMed: 10835623]

Sar M, Welsch F. Differential expression of estrogen receptor-beta and estrogen receptor-alpha in the rat ovary. Endocrinology. 1999; 140:963–971. [PubMed: 9927330]

Shapiro E, Huang H, Masch RJ, McFadden DE, Wu XR, Ostrer H. Immunolocalization of androgen receptor and estrogen receptors alpha and beta in human fetal testis and epididymis. J Urol. 2005; 174:1695–1698. discussion 1698. [PubMed: 16148684]

Shughrue PJ, Lane MV, Scrimo PJ, Merchenthaler I. Comparative distribution of estrogen receptor-alpha (ER-alpha) and beta (ER-beta) mRNA in the rat pituitary, gonad, and reproductive tract. Steroids. 1998; 63:498–504. [PubMed: 9800279]

Soriano P. Generalized lacZ expression with the ROSA26 Cre reporter strain. Nat Genet. 1999; 21:70–71. [PubMed: 9916792]

Thomason LC, Sawitzke JA, Li X, Costantino N, Court DL. Recombineering: genetic engineering in bacteria using homologous recombination. Curr Protoc Mol Biol. 2014; 106:1 16 11–11 16 39. [PubMed: 24733238]

Tremblay GB, Tremblay A, Copeland NG, Gilbert DJ, Jenkins NA, Labrie F, Giguere V. Cloning, chromosomal localization, and functional analysis of the murine estrogen receptor beta. Mol Endocrinol. 1997; 11:353–365. [PubMed: 9058381]

Ulbrich SE, Kettler A, Einspanier R. Expression and localization of estrogen receptor alpha, estrogen receptor beta and progesterone receptor in the bovine oviduct in vivo and in vitro. J Steroid Biochem Mol Biol. 2003; 84:279–289. [PubMed: 12711014]

Valimaa H, Savolainen S, Soukka T, Silvoniemi P, Makela S, Kujari H, Gustafsson JA, Laine M. Estrogen receptor-beta is the predominant estrogen receptor subtype in human oral epithelium and salivary glands. J Endocrinol. 2004; 180:55–62. [PubMed: 14709144]

van Pelt AM, de Rooij DG, van der Burg B, van der Saag PT, Gustafsson JA, Kuiper GG. Ontogeny of estrogen receptor-beta expression in rat testis. Endocrinology. 1999; 140:478–483. [PubMed: 9886860]

Vanderhorst VG, Gustafsson JA, Ulfhake B. Estrogen receptor-alpha and -beta immunoreactive neurons in the brainstem and spinal cord of male and female mice: relationships to monoaminergic, cholinergic, and spinal projection systems. J Comp Neurol. 2005; 488:152–179. [PubMed: 15924341]

Weihua Z, Saji S, Makinen S, Cheng G, Jensen EV, Warner M, Gustafsson JA. Estrogen receptor (ER) beta, a modulator of ERalpha in the uterus. Proc Natl Acad Sci U S A. 2000; 97:5936–5941. [PubMed: 10823946]

Wigglesworth K, Lee KB, O'Brien MJ, Peng J, Matzuk MM, Eppig JJ. Bidirectional communication between oocytes and ovarian follicular somatic cells is required for meiotic arrest of mammalian oocytes. Proc Natl Acad Sci U S A. 2013; 110:E3723–3729. [PubMed: 23980176]

Wu CT, Chang YL, Shih JY, Lee YC. The significance of estrogen receptor beta in 301 surgically treated non-small cell lung cancers. J Thorac Cardiovasc Surg. 2005; 130:979–986. [PubMed: 16214508]

Yamaguchi N, Yuri K. Estrogen-dependent changes in estrogen receptor-beta mRNA expression in middle-aged female rat brain. Brain Res. 2014; 1543:49–57. [PubMed: 24239930]

Yu KD, Rao NY, Chen AX, Fan L, Yang C, Shao ZM. A systematic review of the relationship between polymorphic sites in the estrogen receptor-beta (ESR2) gene and breast cancer risk. Breast Cancer Res Treat. 2011; 126:37–45. [PubMed: 20390341]

Zhao C, Dahlman-Wright K, Gustafsson JA. Estrogen receptor beta: an overview and update. Nucl Recept Signal. 2008; 6:e003. [PubMed: 18301783]

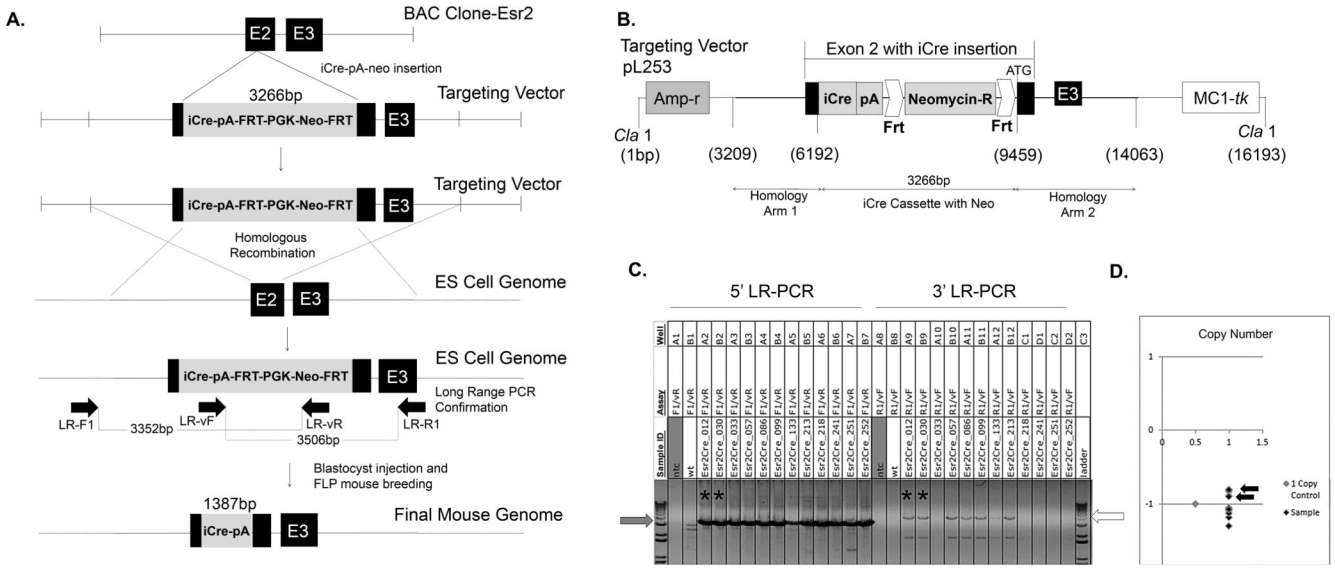

Figure 1. Generation of Esr2-iCre mice

To create mice that faithfully express codon-improved Cre recombinase under regulation of estrogen receptor beta, an iCre-polyA-FRT-PGK-neomycin-FRT cassette was inserted the *Esr2* gene. **A.** First, a targeting vector was generated in a BAC clone by inserting the construct containing iCre into exon 2 [E2] of *Esr2*. Next the targeting vector was inserted into the genome of C57BL/6J embryonic stem cells using homologous recombination; stem cells were screened for correct insertion location and direction by long range PCR and copy number. Horizontal arrows represent LR-PCR primer binding sites. One clone was then used for blastocyst injection to create a knock-in mouse line. One chimeric mouse that gave birth to multiple black iCre-positive offspring was chosen as a founder and one offspring was crossed with a FLP recombinase-expressing mouse to remove the FRT-PGK-neo-FRT targeting vector. **B.** The iCre-polyA-FRT-PGK-neomycin-FRT cassette was inserted into exon 2 of the *Esr2* gene in a BAC clone and retrieved in a pL253 targeting vector. Homology arms allowing for recombination were added to each end of the cassette by restriction enzyme digestion and end joining. The targeting vector was linearized by *Cla*1 digestion and inserted into the genome of C57BL/6J embryonic stem cells. **C.** After homologous recombination, long-range PCR was used to identify ES cell clones that had correct homologous recombination in the 5'-side homology arm of the targeting vector using primers LR-F1 and LR-vR. Positive PCR bands are indicated by the grey arrow in **C**). Among them, six clones had correct homologous recombination in the 3'-side homology as well (white arrow, primers LR-vF and LR-R1). These six clones were further screened to determine whether the iCre sequence was additionally inserted somewhere else in the genome. Two clones (asterisks corresponding to arrows in **D**) had one cassette insertion at the correct location and orientation. **D**. Selection cassette copy number analysis using the neomycin positive marker was used to determine the number of copies of cassette present in each sample and eliminate those with insertions into the genome in addition to the correct location. Two of the clones (black arrows) had a single correct cassette insertion and EsrCre_030 was ultimately used for blastocyst injection.

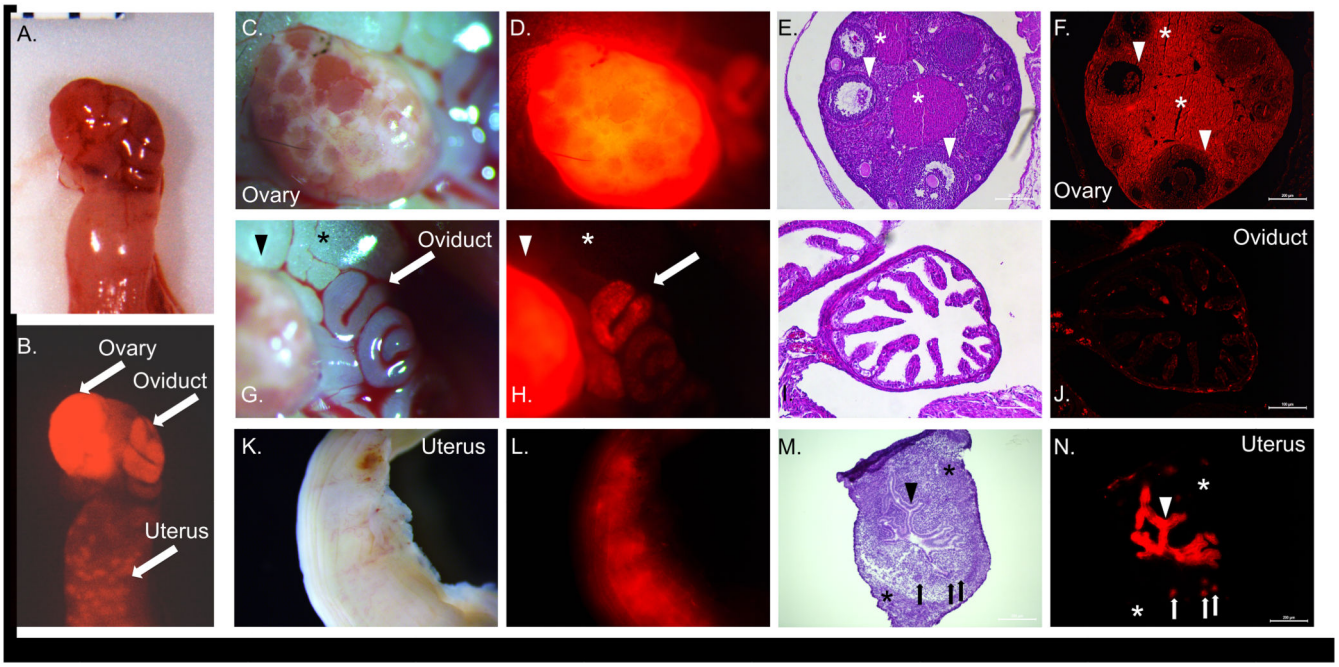

Figure 2. Expression of Esr2-iCre in the ovary, oviduct, and uterus

Female reproductive organs from post-natal day 60 female Esr2-iCre Ai9 mice were collected; mice were unstimulated and had not previously been pregnant. **A,B** Fluorescence was grossly observed in the ovary, oviduct, and uterus. **C-F** Strongest fluorescence was seen throughout the ovary, in the granulosa cells as well as the lutein cells of the corpora lutea and the stromal cells. A few oocytes (~5%) within mature follicles are RFP positive. Arrowhead: antral follicle; asterisk: corpus luteum. **G-J** Punctate fluorescence was seen in the oviduct, particularly in the proximal oviduct (ampulla). Fluorescence was limited to individual epithelial cells. Arrow: oviduct; arrowhead: ovary; asterisk: adipose tissue. **K-N** In the uterus, diffuse fluorescence was grossly observed throughout. Expression was observed in luminal epithelial cells lining the endometrium and uterine glands (frozen section). Some mice (>60 days) also displayed fluorescence in the several individual endometrial stromal cells and myometrial smooth muscle cells. Arrowhead: luminal epithelium; asterisk: myometrium; arrow: glandular epithelium. Magnification: **E,F**: 10×; **I,J**: 20×; **M,N**: 10×.

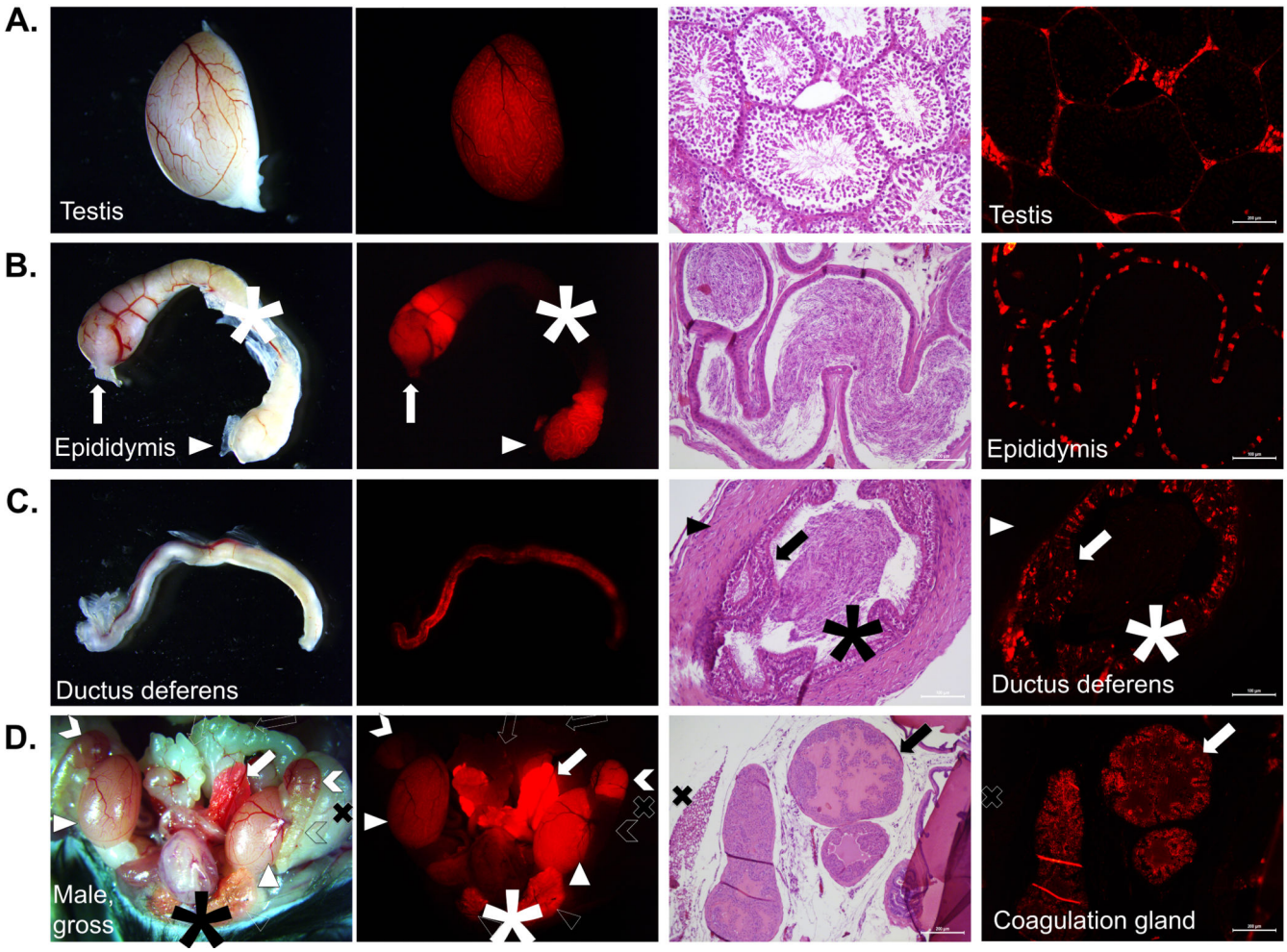

Figure 3. Functional expression of Esr2-iCre in the male gonad and accessory organs

Mature post-natal day 60 male Esr2i-iCre Ai9 mice were sacrificed and organs were collected for histology. **A.** In the testis, fluorescence was grossly visible outlining the individual seminiferous tubules but not vessels or adipose tissue. Histologically, fluorescence was observed in interstitial cells including Leydig cells but not Sertoli cells or any germ cells (10×). **B.** The head and tail (caput and cauda) of the epididymis but not the body (corpus) were RFP-positive. Cells of the epididymal epithelium stained in an individual punctate pattern with no fluorescence observed in the smooth muscle cells or the spermatozoa (cauda epididymis, 20×). Arrow: caput; asterisk: corpus; arrowhead: cauda. **C.** There was weak and scattered staining grossly throughout the ductus deferens. Histologically, fluorescence was limited to a punctate or stippled pattern in only the epithelial cells, similar to the epididymis. Arrow: epithelium; asterisk: spermatozoa; arrowhead: smooth muscle; 20×. **D.** Grossly after opening the peritoneal cavity, obvious fluorescence was observed in the testis, prepucial gland, caput and cauda epididymis, and was brightest in the anterior prostate/coagulation gland, with weaker fluorescence in the ductus deferens and bladder. No fluorescence was observed in the seminal vesicles, the ureters, or the body of the epididymis. The epithelial cells of the coagulation gland were RFP-positive on histological examination (10×). Solid arrow: coagulation gland; open

arrow: seminal vesicle: solid arrowhead: testis; open arrowhead: prepucial gland (cut); solid chevron: caput epididymis; open chevron: corpus epididymis; asterisk: bladder.

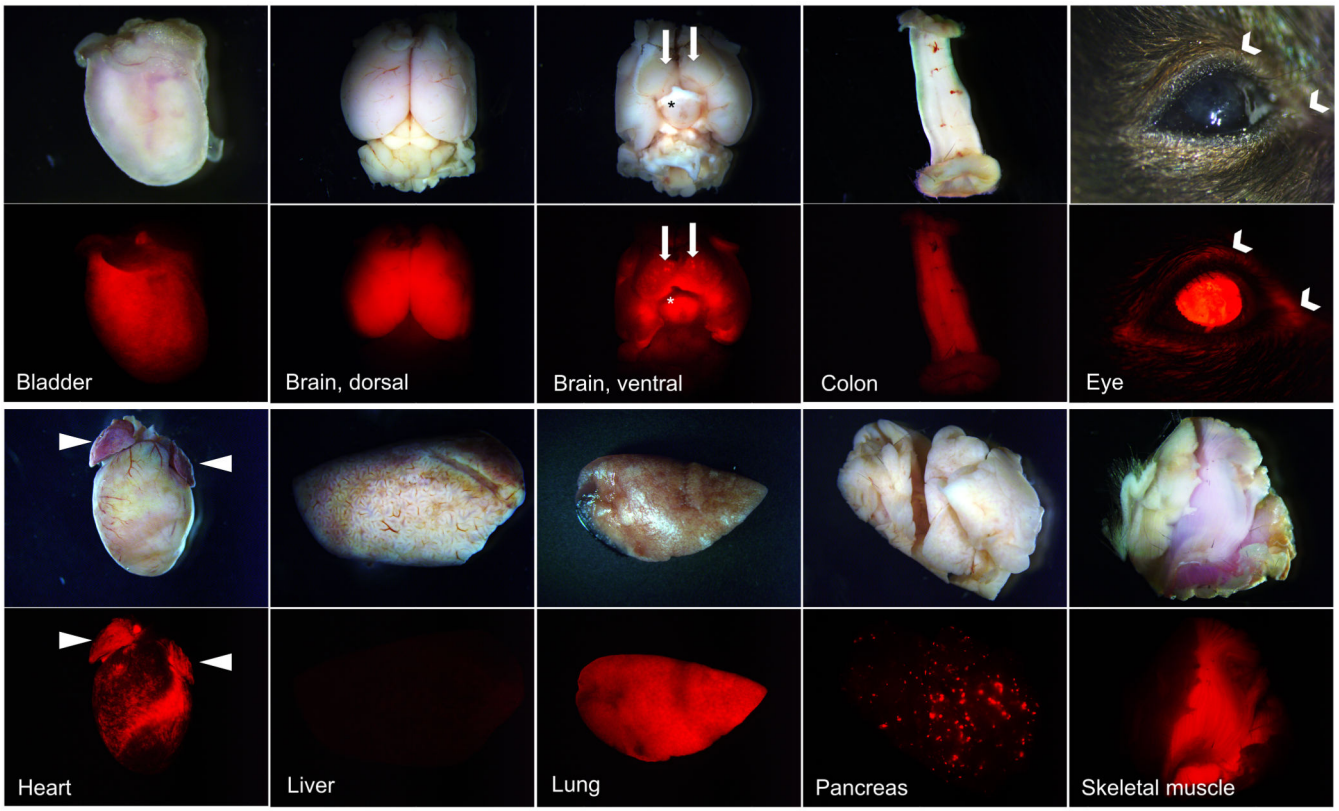

Figure 4. Expression of Esr2-iCre throughout the body

Esr2-iCre Ai9 mouse tissues were collected at 2-4 months of age. Expression was similar in the organs of mice of each gender, including the brain and pituitary. Consistent faint fluorescence was observed throughout the detrusor muscle of the bladder. In the brain, neurons of the cerebrum were RFP-positive though this was sharply limited to the forebrain. Ventrally, expression was present throughout the hypothalamus (asterisk) and the ventral portion of the cerebrum; expression was absent from the optic nerve chiasm. Uniquely, expression was observed in bilaterally symmetrical ventral point structures about the olfactory tubercle (solid arrows, ventral brain view). The mucosa of the distal GI tract (colon, cecum), the central interior cornea of the eyes and the nearby conjunctiva (chevron), the epicardium surrounding the coronary arteries and atria of the heart (arrowheads), the entirety of the lungs, select acini of the pancreas, and throughout the skeletal muscle of the body (skeletal muscle in center surrounded by adipose tissue and skin).

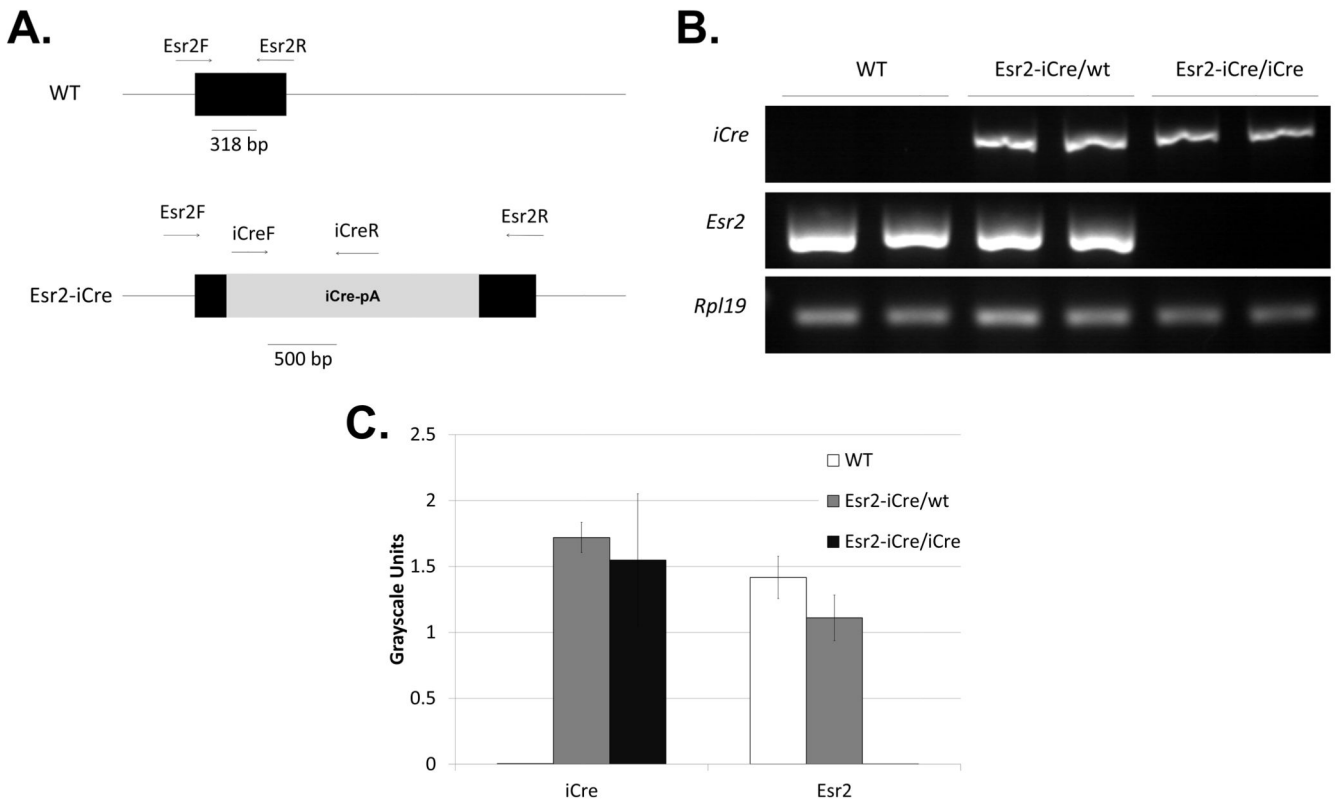

Figure 5. Esr2-iCre homozygous mice globally lack *Esr2*

Esr2-iCre mice were bred together to generate mice homozygous for the iCre allele. Female mice were sacrificed at 26 days old and ovaries were collected. **A.** The primer locations and band size for Esr2 forward and reverse primers and iCre forward and reverse primers are shown for WT and Esr2-iCre mice. **B.** Semi-quantitative PCR revealed no *Esr2* expression in homozygous iCre mice, and there was no difference in *Esr2* expression in heterozygous Esr2-iCre and WT mice. Similarly, *iCre* expression was not different between heterozygous and homozygous Esr2-iCre mice and was absent in WT mice. Expression of *iCre* mimics *Esr2*. *Rpl19* was used as an internal control. **C.** Quantitative expression was determined by semi-quantitative PCR based on band intensity; n=4/group, error bars represent the S.E.M.

Table 1

Summary of Esr2-iCre expression in adult mice

Expression was visualized in multiple tissues in adult Esr2-iCre Ai9 intact mice (60+ days of age) through RFP signaling. Fluorescence marks cells that may be expressing Cre recombinase or cells that previously have, or have emerged from a cell lineage with a progenitor cell that had expressed Cre.

Tissue	Relative Fluorescence	Notes	Select Relevant Literature
Adipose Tissue	−	No fluorescence visualized.	(Gao and Dahlman-Wright, 2013; Pedersen *et al.*, 2001; Tomicek *et al.*, 2011)
Adrenal	++	Punctate or streaked fluorescence throughout the three layers of the adrenal cortex; little to none in medulla.	(Georgiadou *et al.*, 2008; Khasar *et al.*, 2005)
Aorta	−	Limited fluorescence to skeletal muscle near aorta.	(Darblade *et al.*, 2002; Li *et al.*, 2011)
Bladder	+	Diffuse, weak fluorescence throughout the detrusor muscle.	(Elicevik *et al.*, 2006; Imamov *et al.*, 2007; Krege *et al.*, 1998; Kuiper *et al.*, 1997)
Blood (circulating)	−	No fluorescence seen (in all RBC and WBCs observed).	(Lamote *et al.*, 2007; Stygar *et al.*, 2007)
Bone (femur)	−	No fluorescence seen in osteocytes, bone marrow.	(Moverare *et al.*, 2004; Okazaki *et al.*, 2002)
Brain	++	Diffuse fluorescence throughout cerebrum and hypothalamus; none in optic chiasm, cerebellum, or hind brain. Marked increased fluorescence at several small points on the ventral surface.	(Hrabovszky *et al.*, 2004; Isgor *et al.*, 2003; Isgor *et al.*, 2002; Weiser *et al.*, 2008; Yu *et al.*, 2010)
Coagulation gland (anterior prostate)	+++	Strong fluorescence seen in secretory cells.	(Moverare *et al.*, 2004)
Colon	++	Diffuse to patchy fluorescence throughout mucosa, stronger and more widespread than in proximal GI tract.	(Hasson *et al.*, 2014; Levin, 2009)
Ductus (vas) deferens	+	Limited, punctate fluorescence in some luminal epithelial cells; weaker than head and tail of epididymis.	(Atanassova *et al.*, 2001)
Duodenum	+	Limited punctate fluorescence in mucosa and stroma of the submucosa. More points of expression are visible at the more distal portion.	(Kawano *et al.*, 2004)
Epididymis	++	Strong fluorescence seen in the epithelium of the tubules connecting to the rete and in the head of the epididymis. No fluorescence in the body of the epididymis. Fluorescence again present in the epithelium of the tail of the epididymis.	(Cooke *et al.*, 1991; Hess *et al.*, 1997; Shapiro *et al.*, 2005)
Esophagus	−	No fluorescence visualized.	(Akgun *et al.*, 2002)
Eye	+	Fluorescence visible in the most interior cellular layer of	(Cammarata *et al.*, 2005; Flynn

Tissue	Relative Fluorescence	Notes	Select Relevant Literature
		the cornea, not present in the lens or retina.	*et al.*, 2008)
Heart	++	Patchy fluorescence in some of the epicardial cells, particularly those near the coronary arteries or surface adipose deposits. Fluorescence also present throughout majority of the myocardial cells of each atrium.	(Babiker *et al.*, 2006; Kararigas *et al.*, 2014; Pelzer *et al.*, 2005)
Ileum	+	Limited punctate fluorescence in mucosa and submucosa similar to the duodenum, stronger distally.	(Kawano *et al.*, 2004)
Jejunum	+	Limited punctate fluorescence in mucosa and submucosa similar to duodenum and ileum.	(Kawano *et al.*, 2004)
Kidney	+	Little fluorescence visualized, limited to cortex and particularly in some glomeruli when present.	(Esqueda *et al.*, 2007; Yu *et al.*, 2013)
Liver	−	No fluorescence visualized.	(Iavarone *et al.*, 2003; Paquette *et al.*, 2007; Warner and Gustafsson, 2015)
Lung	+++	Strong fluorescence throughout entirety of lungs and respiratory epithelium.	(Rodriguez-Lara *et al.*, 2014; Song *et al.*, 2013; Zhang *et al.*, 2010)
Nerve (thoracic vagus)	−	No fluorescence visualized.	(Vanderhorst *et al.*, 2005)
Ovary	+++	Fluorescence seen throughout ovary, including granulosa cells, theca cells, stromal cells, and epithelial cells. Not seen in oocytes.	(Choi *et al.*, 2001; Drummond and Fuller, 2012; Jefferson *et al.*, 2000; Krege *et al.*, 1998; O'Brien *et al.*, 1999)
Oviduct	+	Punctate fluorescence in epithelial folds of the proximal oviduct (ampulla). Fluorescence diminished or not present in distal oviduct (isthmus).	(Ulbrich *et al.*, 2003)
Pancreas	++	Fluorescence present in endocrine pancreas only within some of the pancreatic acini, approximately 5%.	(Morales *et al.*, 2003)
Penis	−	No fluorescence visualized externally.	(Jesmin *et al.*, 2002)
Peyers Patch (Gut-associated lymphatic tissue)	+	Very limited punctate expression visualized within follicles, 0-2 lymphocytes/100.	
Pituitary	++	Fluorescence visible throughout cells of the posterior pituitary, none visible in intermediary pituitary, punctate or diffuse expression in medial anterior pituitary with decreased prevalence near lateral edges.	(Richards *et al.*, 2002; Shughrue *et al.*, 1998; Wilson *et al.*, 1998)
Preputial gland	+++	Fluorescence seen in the majority of acini in both basal and secretory cells.	
Salivary gland	++	Fluorescence present throughout the serous cells of acini, overall spotted pattern histologically.	(Ohshiro *et al.*, 2006; Valimaa *et al.*, 2004)
Seminal vesicle	−	No fluorescence visualized	

Tissue	Relative Fluorescence	Notes	Select Relevant Literature
Skeletal muscle	+++	Obvious, strong fluorescence throughout skeletal muscle throughout the body.	(Glenmark *et al.*, 2004; Milanesi *et al.*, 2009; Velders *et al.*, 2012)
Skin	±	Fluorescence limited to 1-2 cells/hair follicle, otherwise not seen histologically in skin; fluorescence also present on pads of feet.	(Krahn-Bertil *et al.*, 2010; Markiewicz *et al.*, 2013; Ohata *et al.*, 2008)
Spleen	−	No fluorescence visualized.	(Hildebrand *et al.*, 2006)
Stomach	−	No fluorescence visualized.	(Campbell- Thompson *et al.*, 2001; Wakui *et al.*, 2011)
Testes	++	Strong fluorescence in interstitial cells, including Leydig cells; not present in Sertoli cells of seminiferous tubules; punctate expression in epithelium lining the rete.	(Choi *et al.*, 2001; Hess *et al.*, 1997; Pearl *et al.*, 2011; van Pelt *et al.*, 1999)
Uterus	+	Seen in epithelial and some stromal cells of the endometrium, and some smooth muscle cells of the myometrium and throughout the uterus.	(Dupont *et al.*, 2000; Kang *et al.*, 2003; Minorics *et al.*, 2004; Pastore *et al.*, 2012)
Vagina	+	Expression seen in the stratified mucosa of vagina in cycling adult mice.	(Kang *et al.*, 2003)